

Enabling infinite Q factors in absorbing optical systems

Radoslaw Kolkowski* and Andriy Shevchenko†

Department of Applied Physics, Aalto University, P.O.Box 13500, Aalto FI-00076, Finland

(Dated: April 27, 2023)

Resonant optical systems have widespread applications in science and technology. However, their quality (Q) factors can be significantly deteriorated, if some of their parts exhibit optical absorption. Here, we show that by coupling a lossy mode of such a structure to two independent lossless modes, one can create a nonradiating and absorption-free bound state in the continuum (BIC). The Q factor of such a BIC is theoretically unlimited despite interaction with an absorbing structure. We use this mechanism to design a plasmonic metasurface with Q factors that are close to 10^7 in the visible spectral range. The proposed mechanism is general and can be used to engineer ultrahigh- Q resonances in various absorbing structures.

I. INTRODUCTION

Resonant optical systems are an essential part of modern science and technology, enabling the operation of lasers and providing the means for controlling various light-matter interactions. The main parameter describing such systems is the Q factor, which quantifies the average amount of time each photon spends trapped inside the resonator before it either escapes or gets absorbed. Recently, the concept of bound states in the continuum (BICs) has provided an efficient strategy for eliminating the radiation loss [1, 2], making it possible to realize high- Q resonances in a diverse variety of non-absorbing optical systems [3, 4], including photonic crystals [5, 6], metasurfaces [7–10], and individual dielectric nanoresonators [11, 12]. The highest Q factors of BICs achieved in such non-absorbing systems are on the order of 10^5 - 10^6 [13, 14], which is not far from the state-of-the-art photonic crystal cavities that can achieve Q factors on the order of 10^7 [15, 16]. Therefore, optical BICs have been considered promising for a range of applications [17–20], e.g., in laser technology [21–26] and nonlinear optics [27–30].

However, structures made of absorbing materials have always been regarded as detrimental to the Q factors and not suitable for ultrahigh- Q systems [31], unless absorption can be compensated for by gain [32]. This is because destructive interference in the far-field reduces the radiation loss, but the absorption loss remains unaffected, if not increased [33–36]. On the other hand, absorption can be suppressed via destructive interference in the near-field [37–39], which typically occurs under different conditions than those required by BICs. This has been the reason for relatively modest Q factors, on the order of 10^2 - 10^3 , achieved by BICs in plasmonic and hybrid plasmonic-dielectric structures [40–50]. Consequently, absorbing materials, such as metals and some high-index semiconductors have been avoided when realizing BICs and other types of ultrahigh- Q resonators,

despite the fact that these materials can be very efficient in controlling optical fields [51–53].

In this work, we discover a simple and general mechanism leading to a BIC in which *both* the radiation and absorption losses are eliminated. Such a BIC can be realized by coupling the lossy oscillator to two initially lossless optical modes. The losses due to both the radiation and absorption are *simultaneously suppressed* when the two lossless modes have equal resonance frequencies. There are no explicit symmetry requirements for the coupled modes as long as the coupling mechanism is preserved. This makes the presented BIC very general compared to other types of BICs that are subject to various symmetry constraints. Destructive interference of the coupled modes makes the underlying mechanism similar to the previously studied Friedrich-Wintgen BICs [54] that have been observed in systems with avoided crossings [41, 45–47, 55, 56]. Some of these systems exhibited a reduction of the absorption loss [56]. However, the possibility to completely eliminate the absorption loss together with the radiation loss has not been in the focus of previous works.

Using numerical simulations, we demonstrate the existence of such BICs in a realistic physical system – a periodic metasurface composed of a slab waveguide and an array of metal nanoparticles [57, 58]. By this example, we show that the proposed BICs can originate from modes of different types, such as TE and TM guided modes. In this case, the coupling results in a BIC with a mixed TE-TM polarization state. The hybrid resonances we introduce here can be perfectly lossless, even though the coupling of the modes is provided by lossy nanostructures. Our findings suggest that even strongly absorbing plasmonic or semiconductor materials can be used to construct ultrahigh- Q resonant systems based on BICs. The unique properties of such materials, combined with those of BICs, can lead to superior photonic devices with new functionalities.

* radoslaw.kolkowski@aalto.fi

† andriy.shevchenko@aalto.fi

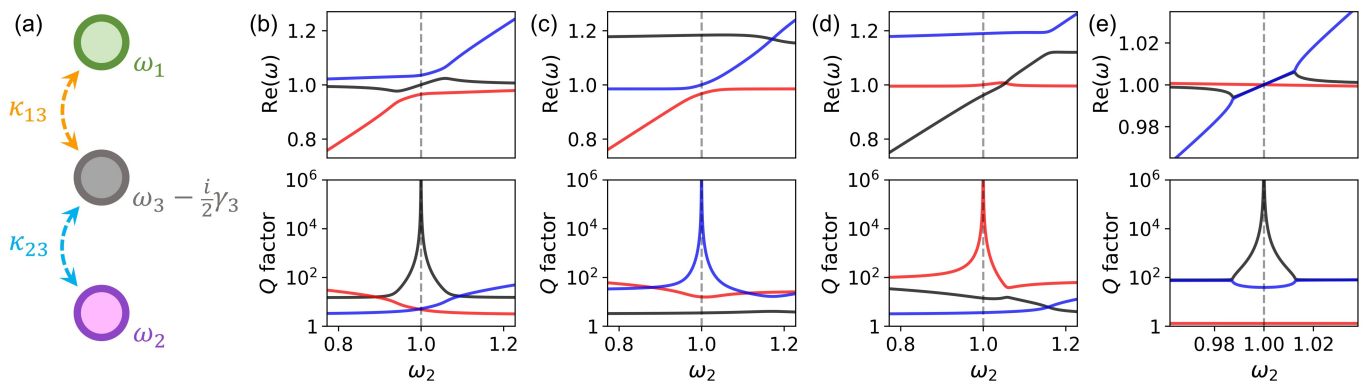


FIG. 1. (a) Illustration of the coupling between three oscillators described by Hamiltonian \mathbf{H} in Eq. (2). The plots in (b)-(e) show the real parts of the complex eigenvalues ω (top) and the corresponding Q factors ($Q = \frac{1}{2} \text{Re}(\omega)/\text{Im}(\omega)$, bottom) of the eigenstates of Hamiltonian \mathbf{H} , as functions of the resonance frequency ω_2 . The plots in (b) show the resonant case ($\omega_3 = \omega_1$) in which the BIC coincides with the lossy resonance, whereas (c) and (d) correspond to the off-resonant scenario ($\omega_3 = 1.15\omega_1$). The plots in (e) correspond to a strongly non-Hermitian system (with $\omega_3 = \omega_1$) in which the BIC is accompanied by a pair of exceptional points instead of an avoided crossing. In all plots, $\omega_1 = 1$, whereas the other parameters are: $\kappa_{13} = \kappa_{23} = 0.075$ and $\gamma_3 = 0.2$ in (b) and (c), $\kappa_{13} = 0.045$, $\kappa_{23} = 0.105$ and $\gamma_3 = 0.2$ in (d), and $\kappa_{13} = \kappa_{23} = 0.05$ and $\gamma_3 = 0.4$ in (e).

II. MECHANISM OF LOSS CANCELLATION

Consider a system of coupled harmonic oscillators described by the following equations:

$$\frac{d^2 x_p}{dt^2} + \gamma_p \frac{dx_p}{dt} + \omega_p^2 x_p - \sum_{q \neq p} \Omega_{pq}^2 x_q = 0, \quad (1)$$

where x_p is the instantaneous amplitude of a p^{th} oscillator, γ_p the damping rate, ω_p the resonance frequency, and Ω_{pq} the coupling rate between the oscillators p and q . Assuming the ansatz $x_p = x_{p,0} e^{-i\omega t}$ and using the approximation $|\omega_p - \omega| \ll \omega$, the above set of equations can be simplified into a linear eigenvalue problem [59]: $\det(\mathbf{H} - \omega \mathbf{I}) = 0$. Here, \mathbf{I} is the identity matrix, whereas the Hamiltonian \mathbf{H} has the diagonal terms $\omega_p - \frac{i}{2}\gamma_p$ and off-diagonal terms $\kappa_{pq} = \frac{1}{2}\Omega_{pq}^2/\bar{\omega}$ with $\bar{\omega} \approx (\omega + \omega_p)/2$.

Now, consider a system composed of two oscillators with resonance frequencies ω_1 and ω_2 that are not directly coupled to each other ($\kappa_{12} = 0$) and show no losses ($\gamma_1 = \gamma_2 = 0$). Next, we introduce a third oscillator with resonance frequency ω_3 and damping rate γ_3 coupled to the first and second oscillators via κ_{13} and κ_{23} , respectively [see Fig. 1(a)]. This system of oscillators is described by the Hamiltonian

$$\mathbf{H} = \begin{pmatrix} \omega_1 & 0 & -\kappa_{13} \\ 0 & \omega_2 & -\kappa_{23} \\ -\kappa_{13} & -\kappa_{23} & \omega_3 - \frac{i}{2}\gamma_3 \end{pmatrix}. \quad (2)$$

In the context of optical resonances, the eigenstates of this Hamiltonian are quasi-normal modes [60–62] associated with complex eigenvalues ω , where $\text{Im}(\omega)$ describes the losses. A somewhat similar three-mode system has been considered as a generalization to the Friedrich-Wintgen BIC [46, 63] and as a classical analog of the dou-

ble electromagnetically induced transparency [64]. Solving the eigenvalue problem yields the following relation:

$$(\omega_1 - \omega)(\omega_2 - \omega)(\omega_3 - \frac{i}{2}\gamma_3 - \omega) = \kappa_{23}^2(\omega_1 - \omega) + \kappa_{13}^2(\omega_2 - \omega). \quad (3)$$

For $\omega_1 = \omega_2$, this equation can be written as

$$(\tilde{\omega} - \omega)^2(\omega_3 - \frac{i}{2}\gamma_3 - \omega) = (\kappa_{13}^2 + \kappa_{23}^2)(\tilde{\omega} - \omega), \quad (4)$$

where $\tilde{\omega} = \omega_1 = \omega_2$. The above relation clearly shows that the system under consideration hosts a lossless hybrid eigenstate at $\omega = \tilde{\omega}$ that is fully independent of the elements κ_{13} , κ_{23} , and $\omega_3 - \frac{i}{2}\gamma_3$. Most importantly, this eigenstate is completely immune to losses expressed by γ_3 , which may include also the absorption loss. This is in contrast to the Friedrich-Wintgen BIC emerging from two resonances with radiation losses only [1, 54].

The appearance of a lossless BIC in the above system is illustrated in Fig. 1(b)-(e), where the eigenvalues of \mathbf{H} are plotted as functions of the resonance frequency ω_2 . The BIC is present at $\omega_2 = \omega_1$, regardless of the choice of parameters ω_3 , γ_3 , κ_{13} , and κ_{23} . In particular, Fig. 1(b) shows the resonant scenario ($\omega_1 = \omega_3$), whereas in Fig. 1(c), the lossy resonance of frequency ω_3 is strongly detuned from ω_1 . The BIC would also emerge if the rest of the parameters was chosen differently, giving rise to hybrid modes of a qualitatively distinct character. For example, if $\kappa_{13} \neq \kappa_{23}$ or $\kappa_{13/23} \ll \gamma_3$, one can obtain the accidental degeneracies and exceptional points [47, 65] in addition to the BIC, which is illustrated in Figs. 1(d) and 1(e).

A relatively similar mechanism to eliminate absorption is that of the electromagnetically induced transparency [66, 67]. In our case, however, the loss cancellation occurs by interference of three excited modes instead of two driving fields. Similarly, in the symmetry-protected

BICs [7, 68, 69] and Friedrich-Wintgen BICs [41, 45–47, 55, 56], the modes can exhibit a reduced absorption loss due to their local interference in the near-field, that can be destructive to some degree [46, 56]. However, the coupling mechanism presented here ensures that simultaneous cancellation of the radiation and absorption losses depends only on the frequency matching of the modes and takes place without any specific symmetry requirements, as long as the coupling mechanism is retained.

The proposed mechanism can be implemented in various physical systems. One of them is a linear array of coupled waveguides. In a configuration of three parallel waveguides, the middle one can be lossy, while the other two lossless. If the two side waveguides are coupled only through the central waveguide, then the propagation of light in the array can be described by the same Hamiltonian as in Eq. (2). The main difference between the coupled waveguides and coupled oscillators is that, in the case of coupled waveguides, the eigenvalues ω should be interpreted as the propagation constants of the eigenmodes, and not as their eigenfrequencies. One eigenmode, in which absorption is eliminated, has an antisymmetric field distribution with zero amplitude in the middle waveguide and out-of-phase oscillation in the side waveguides [70]. This eigenmode would propagate without losses despite the fact that the two waveguides on the sides are coupled through the lossy waveguide.

A slightly more complex optical system that realizes the proposed mechanism would be a system of three coupled ring resonators, in which the central resonator is lossy. One may expect an eigenmode, in which light is trapped in the two lossless resonators, avoiding the lossy one. However, the coupling would still occur through the lossy resonator, locking the relative phase of the fields in the lossless resonators. The fields of the two coupled modes in the lossy resonator will disappear due to destructive interference. Other types of optical resonators can also be considered, e.g., Fabry-Pérot cavities [71], photonic crystal cavities [72], antenna-cavity hybrids [73–75], optomechanical resonators [76], and elementary quantum oscillators, such as atoms and molecules [77]. The presented BIC would also have analogs in physical systems beyond optics, e.g., in purely mechanical oscillators (starting with the classic example of coupled pendulums), acoustic resonators [78], and electric circuits [79].

III. A PLASMONIC METASURFACE

To demonstrate the capabilities of the proposed BIC, we consider a periodic metasurface composed of a 2D array of metal nanoparticles on the surface of a lossless slab waveguide [see Fig. 2(a)]. We assume that the metasurface is sufficiently large, such that it can be described using periodic boundary conditions with the in-plane momentum \mathbf{k}_{\parallel} . Hybrid optical metasurfaces of this type have been studied previously in the context of plasmonic-photonic resonances known as waveguide-plasmon polar-

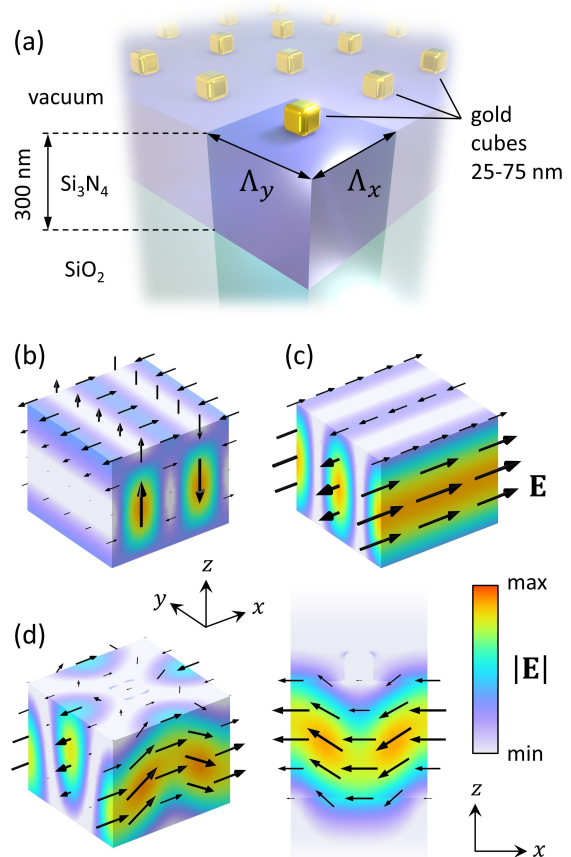


FIG. 2. (a) Schematic illustration of a metasurface supporting hybrid BICs. The unit cell and the two lattice periods Λ_x and Λ_y are highlighted in the foreground. In (b), (c), and (d), the spatial distributions of the electric field norm (color) and instantaneous electric field vector (black arrows) are shown. They were obtained using COMSOL Multiphysics. In (b) and (c), two eigenmodes of a bare Si_3N_4 waveguide at the Γ point are presented: (b) TM mode, forming a standing wave along x with a node in the center of the unit cell; (c) TE mode, forming a standing wave along y with an antinode in the center of the unit cell. (d) A hybrid quasi-BIC excited in a metasurface by normally incident plane wave polarized along x ($\lambda \approx 645.43$ nm, $\Lambda_x = 352.5$ nm, $\Lambda_y = 340$ nm, nanocube size 75 nm): 3D view of the unit cell (on the left) and cross-cut in the xz -plane (on the right).

itons (WPPs) [57, 58]. In this work, we investigate the coupling between the TE and TM modes mediated by an array of lossy nanoparticles, giving rise to a hybrid BIC with suppressed absorption loss rate and a mixed TE-TM polarization state. Obviously, there can be found other coupling configurations for this demonstration, e.g., coupling between TE modes in a square lattice, or coupling between two counter-propagating modes in a simple one-dimensional grating. However, the purpose of the example we have chosen is to show that the proposed BIC can be formed independently of any specific sym-

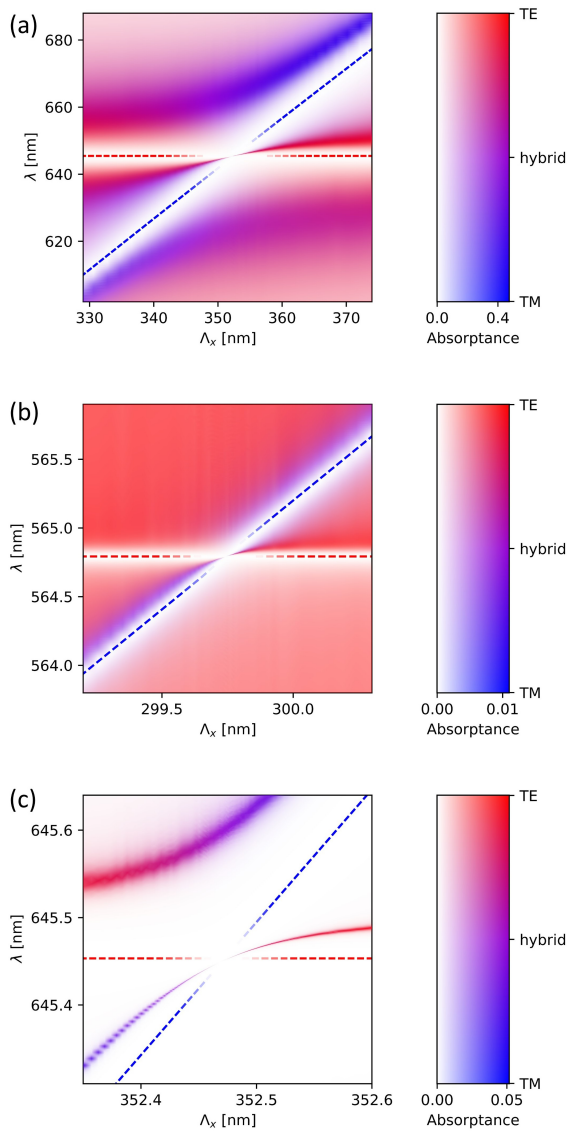


FIG. 3. Hybrid quasi-BICs revealed in metasurfaces with various geometrical parameters. The absorbance and the average polarization state of the excited electric field are plotted as functions of period Λ_x (horizontal axis) and incident wavelength λ (vertical axis). The absorbance is encoded in the opacity of the data points (displayed on a white background), whereas the polarization is encoded in the colors: red for the pure TE polarization, blue for the pure TM polarization, and violet for the hybrid polarization. The red and blue dashed lines illustrate the Bragg condition for the TE and TM guided modes, respectively. These lines are made transparent near the quasi-BICs not to obscure them. The graph in (a) corresponds to metasurfaces with nanocubes of size 75 nm, whereas in the remaining graphs, the size of nanocubes is set to 25 nm. In (b), $\Lambda_y = 292$ nm, whereas in (a) and (c), $\Lambda_y = 340$ nm. In (a) and (b), the quasi-BIC overlaps with the LSPR (a resonant scenario), whereas in (c), the quasi-BIC is away from the LSPR (an off-resonant scenario). The values of absorbance and polarization state were obtained using COMSOL Multiphysics.

metry requirement. The two modes coupled by metal nanoparticles in our example have different polarizations and different field profiles. Moreover, the structure under consideration lacks the up-down mirror symmetry that is required by the Friedrich-Wintgen BICs [55, 80].

In the numerical calculations, the metal nanoparticles are gold nanocubes with the rib size ranging from 25 to 75 nm on the surface of a 300 nm thick waveguide with a Si_3N_4 core and a SiO_2 substrate. The optical constants of Si_3N_4 , SiO_2 , and Au are taken from Refs. [81], [82], and [83], respectively. In fact, the nanoparticle size, shape, and material composition are not critical for the emergence of the proposed BIC and can be chosen arbitrarily. However, we intentionally select nanoparticles that exhibit an electric-dipole-like localized surface plasmon resonance (LSPR) in the visible spectral range, which makes them strongly polarizable by the in-plane polarized evanescent fields of the guided modes. We also deliberately choose gold instead of silver as the nanoparticle material, as it shows significant optical absorption in the visible spectral range. This allows us to demonstrate the efficiency of our approach. In addition, the metasurface design is to some extent driven by the feasibility of its experimental realization and its possible future applications in spectroscopy.

Let us first consider a slab waveguide with a periodic perturbation of infinitesimal strength, i.e., a virtually periodic waveguide in the absence of the nanoparticles. Such a waveguide supports mutually orthogonal TE and TM guided modes described by the effective mode indices n_{TE} and n_{TM} . Due to the periodicity of the system, each of the guided modes forms an onset of standing waves at the Γ point ($|\mathbf{k}_{\parallel}| = 0$). These standing waves correspond to the band edges of the diffractive resonances with resonance frequencies ω governed by the 2nd Bragg condition ($\omega = 2\pi c/n\Lambda$ for the mode index n and lattice period Λ). The resonance frequencies for the TE and TM modes can be matched by tuning the periods along the two lattice directions (x and y), e.g., such that $n_{\text{TE}}\Lambda_y = n_{\text{TM}}\Lambda_x$. By looking at the electric field distributions in Figs. 2(b) and 2(c), one can clearly see that the TM and TE standing waves formed along the x and y axes, respectively, are both polarized parallel to the x -axis at the center of the unit cell on the waveguide surface. Hence, both these modes can resonantly couple to each other through surface-mounted nanoparticles.

The hybridization of the TE and TM standing waves mediated by the nanoparticles gives rise to three new resonances, including a hybrid dark resonance shown in Fig. 2(d). Although in total, there are eight TE and TM standing waves at the Γ point, the contribution of the other modes can be neglected. Hence, the description of the hybrid metasurface under consideration can be based on the Hamiltonian \mathbf{H} of Eq. (2). The TE and TM standing waves can also individually hybridize with the nanoparticles when the system is tuned away from the TE-TM matching condition. In such a case, the hybridization gives rise to simple WPPs.

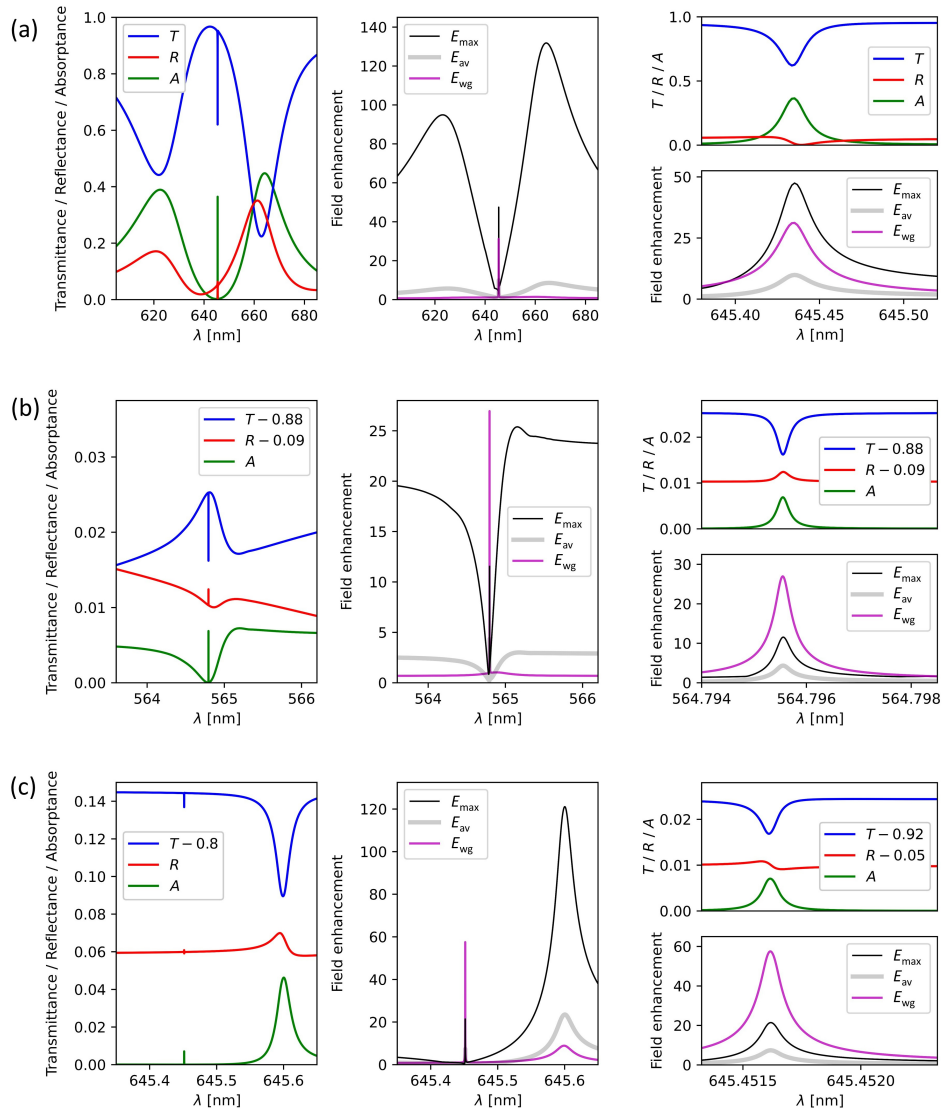


FIG. 4. Spectral dependence of the transmittance (T), reflectance (R), absorptance (A) (left column), and the values of the local field enhancement at the surface of the nanocubes (maximum E_{\max} and average E_{av}) and inside the waveguide (E_{wg}) (middle column). The plots in (a), (b), and (c) reveal the quasi-BICs at $\Lambda_x = 352.5$ nm, 299.75 nm, and 352.47 nm in Figs. 3(a), 3(b) and 3(c), respectively. Graphs in the right column show the magnifications around the quasi-BICs of the graphs in the left and middle column. The values of transmittance, reflectance, absorptance and field enhancement were obtained using COMSOL Multiphysics.

Figure 3 shows the optical properties of the hybrid metasurfaces at normal incidence as a function of period Λ_x and wavelength λ . In particular, Fig. 3(a) shows the anticrossing of the simple TE and TM WPPs (red and blue bands, respectively), resulting in hybrid TE-TM branches (violet) and a high- Q BIC between them. In this case, the intersection of the Bragg conditions for the TE and TM modes (red and blue dashed lines, respectively) overlaps with the LSPR, which makes this scenario similar to that of Fig. 1(b). Due to the relatively large size of the nanoparticles in this example (75 nm), the electric field of the BIC cannot completely avoid the nanoparticles. Despite this, we obtain a rather high

Q factor of 35000, as determined from the full width at half maximum (FWHM) of the absorptance peak in Fig. 4(a). The peak originates from an efficient trapping and strong enhancement of the incident field by the metasurface at the BIC wavelength. The absorption loss rate of light from the system is still highly suppressed, providing a high Q factor. For smaller nanoparticles [Figs. 3(b) and 3(c)], the Q factor can be increased well above 10^6 (up to 2.0×10^6 in the resonant case, and 7.4×10^6 in the off-resonant case), as determined from the peaks in Figs. 4(b) and 4(c). The values of Q factors for various sets of parameters are presented in Fig. 5. The Q factor remains finite as long as the nanoparticles do not

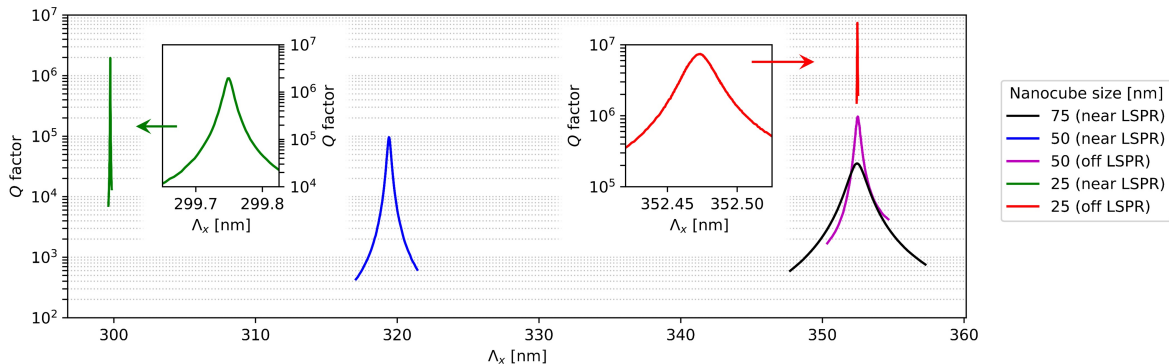


FIG. 5. Q factors of the hybrid quasi-BICs as a function of Λ_x in metasurfaces of various parameters (see legend). The black, green, and red curves correspond to the metasurfaces in Figs. 3(a), 3(b), and 3(c), and Figs. 4(a), 4(b), and 4(c), respectively. Λ_y is set to 340 nm for the black, magenta, and red curves, 310 nm for the blue curve, and 292 nm for the green curve. The curves for 25 nm nanocubes (green and red lines) are magnified in the insets. All values were extracted from the spectral FWHM of the absorbance peaks calculated using COMSOL Multiphysics.

behave as point dipoles. Furthermore, the efficiency of loss cancellation in a real system depends on the validity of the approximations used to derive the Hamiltonian \mathbf{H} in Eq. (2) from Eq. (1). This validity can be affected, e.g., by the contribution of other modes (apart from the three modes considered here), or by the presence of unwanted coupling between the two lossless modes (other than the coupling mediated by the lossy mode). This means that the realizable BICs are *quasi-BICs*, that are able to couple to the incident light, resulting in narrow spectral features, as can be seen in Fig. 4.

The field enhancement spectra in Fig. 4 clearly show that, apart from ultrahigh Q factors, the quasi-BICs can also produce a relatively high local field enhancement, both at the nanoparticle surface and in the waveguide. This is because the high- Q resonance associated with the quasi-BIC allows the light to be efficiently trapped in the metasurface. As a result, its amplitude builds up via constructive interference in all locations, including the lossy nanoparticles that it tries to avoid. Consequently, the interaction of light with the nanoparticles may be strongly enhanced within a narrow resonance band [33–36]. These properties make the presented quasi-BICs very promising for applications in optical sensing [84, 85] and strong light-matter coupling [77]. We emphasize that, in practice, ultrahigh Q factors can be deteriorated by fabrication imperfections, finite illumination area (i.e., finite width of the angular spectrum of the incident beam) [86], and finite lateral extent of the metasurface (side leakage) [13, 87, 88]. However, the proposed BICs are rather insensitive to the geometry of metal nanoparticles, which makes them robust and experimentally feasible compared to typical symmetry-enabled BICs [89].

IV. SUMMARY AND CONCLUSIONS

To summarize, we have demonstrated the possibility of simultaneous suppression of the radiation and absorption

losses in a plasmonic metasurface, creating BICs with Q factors as high as $10^6 - 10^7$, that can be further increased by optimizing the structure (e.g., replacing gold with silver). The presented mechanism of loss cancellation can be implemented in any system of two initially uncoupled and lossless oscillators interacting with a third oscillator that can have arbitrary losses. In this case, the condition for achieving an absorption-free BIC corresponds to the exact matching between the resonance frequencies of the two lossless oscillators. In the example system – a slab waveguide and an array of plasmonic nanoparticles – the TE and TM guided modes played the role of the two lossless oscillators, while the LSPR of the plasmonic nanoparticles served as the third lossy oscillator. The presented mechanism is not limited to the above specific example and can be realized in other physical systems within and beyond optics.

In the context of optical BICs, simultaneous elimination of both the radiation and absorption losses could open up many possibilities. In plasmonics, for example, it could enable high- Q resonances with strong local field enhancement, improving the performance of plasmonic systems [42, 90, 91]. On the other hand, high-index dielectrics (e.g., Si, Ge, and GaAs), which are strongly absorbing in the visible spectral range, could be used to create high- Q Mie-resonant photonic structures [92]. This can be very useful in all applications relying on resonant enhancement of light-matter interaction, including ultrasensitive spectroscopic devices, nonlinear optical modulators and frequency converters, and light emitters with tailored characteristics [93–95].

ACKNOWLEDGMENTS

The authors acknowledge the support of the Academy of Finland (Grants No. 347449 and 353758) and the Flagship of Photonics Research and Innovation (PREIN) funded by the Academy of Finland (Grant No. 320167).

For computational resources, the authors acknowledge the Aalto University School of Science “Science-IT” project and CSC – IT Center for Science, Finland.

DISCLOSURES

The authors declare no conflicts of interest.

DATA AVAILABILITY

Data underlying the results presented in this paper and their replication instructions are openly available at <https://doi.org/10.23729/cfe98559-2ca5-43c6-b8f3-b542f9ff94bb>, Ref. [96].

-
- [1] C. W. Hsu, B. Zhen, A. D. Stone, J. D. Joannopoulos, and M. Soljačić, Bound states in the continuum, *Nature Reviews Materials* **1**, 1 (2016).
- [2] K. Koshelev, G. Favraud, A. Bogdanov, Y. Kivshar, and A. Fratallocchi, Nonradiating photonics with resonant dielectric nanostructures, *Nanophotonics* **8**, 725 (2019).
- [3] D. Marinica, A. Borisov, and S. Shabanov, Bound states in the continuum in photonics, *Physical Review Letters* **100**, 183902 (2008).
- [4] K. Koshelev, A. Bogdanov, and Y. Kivshar, Meta-optics and bound states in the continuum, *Science Bulletin* **64**, 836 (2019).
- [5] C. W. Hsu, B. Zhen, J. Lee, S.-L. Chua, S. G. Johnson, J. D. Joannopoulos, and M. Soljačić, Observation of trapped light within the radiation continuum, *Nature* **499**, 188 (2013).
- [6] H. M. Doeleman, F. Monticone, W. den Hollander, A. Alù, and A. F. Koenderink, Experimental observation of a polarization vortex at an optical bound state in the continuum, *Nature Photonics* **12**, 397 (2018).
- [7] K. Koshelev, S. Lepeshov, M. Liu, A. Bogdanov, and Y. Kivshar, Asymmetric metasurfaces with high-Q resonances governed by bound states in the continuum, *Physical Review Letters* **121**, 193903 (2018).
- [8] A. C. Overvig, S. C. Malek, and N. Yu, Multifunctional nonlocal metasurfaces, *Physical Review Letters* **125**, 017402 (2020).
- [9] A. Overvig and A. Alù, Diffractive nonlocal metasurfaces, *Laser & Photonics Reviews* **16**, 2100633 (2022).
- [10] Z. Li, L. Zhou, Z. Liu, M. Panmai, S. Li, J. Liu, and S. Lan, Modifying the quality factors of the bound states in the continuum in a dielectric metasurface by mode coupling, *ACS Photonics* **10**, 206 (2022).
- [11] M. V. Rybin, K. L. Koshelev, Z. F. Sadrieva, K. B. Samusev, A. A. Bogdanov, M. F. Limonov, and Y. S. Kivshar, High-Q supercavity modes in subwavelength dielectric resonators, *Physical Review Letters* **119**, 243901 (2017).
- [12] A. A. Bogdanov, K. L. Koshelev, P. V. Kapitanova, M. V. Rybin, S. A. Gladyshev, Z. F. Sadrieva, K. B. Samusev, Y. S. Kivshar, and M. F. Limonov, Bound states in the continuum and Fano resonances in the strong mode coupling regime, *Advanced Photonics* **1**, 016001 (2019).
- [13] J. Jin, X. Yin, L. Ni, M. Soljačić, B. Zhen, and C. Peng, Topologically enabled ultrahigh-Q guided resonances robust to out-of-plane scattering, *Nature* **574**, 501 (2019).
- [14] Z. Chen, X. Yin, J. Jin, Z. Zheng, Z. Zhang, F. Wang, L. He, B. Zhen, and C. Peng, Observation of miniaturized bound states in the continuum with ultra-high quality factors, *Science Bulletin* **67**, 359 (2022).
- [15] H. Sekoguchi, Y. Takahashi, T. Asano, and S. Noda, Photonic crystal nanocavity with a Q-factor of ~ 9 million, *Optics Express* **22**, 916 (2014).
- [16] T. Asano, Y. Ochi, Y. Takahashi, K. Kishimoto, and S. Noda, Photonic crystal nanocavity with a Q factor exceeding eleven million, *Optics Express* **25**, 1769 (2017).
- [17] S. I. Azzam and A. V. Kildishev, Photonic bound states in the continuum: from basics to applications, *Advanced Optical Materials* **9**, 2001469 (2021).
- [18] A. S. Kupriianov, Y. Xu, A. Sayanskiy, V. Dmitriev, Y. S. Kivshar, and V. R. Tuz, Metasurface engineering through bound states in the continuum, *Physical Review Applied* **12**, 014024 (2019).
- [19] T. Shi, Z.-L. Deng, G. Geng, X. Zeng, Y. Zeng, G. Hu, A. Overvig, J. Li, C.-W. Qiu, A. Alù, *et al.*, Planar chiral metasurfaces with maximal and tunable chiroptical response driven by bound states in the continuum, *Nature Communications* **13**, 4111 (2022).
- [20] S. C. Malek, A. C. Overvig, A. Alù, and N. Yu, Multifunctional resonant wavefront-shaping meta-optics based on multilayer and multi-perturbation nonlocal metasurfaces, *Light: Science & Applications* **11**, 246 (2022).
- [21] S. T. Ha, Y. H. Fu, N. K. Emani, Z. Pan, R. M. Bakker, R. Paniagua-Domínguez, and A. I. Kuznetsov, Directional lasing in resonant semiconductor nanoantenna arrays, *Nature Nanotechnology* **13**, 1042 (2018).
- [22] A. Kodigala, T. Lepetit, Q. Gu, B. Bahari, Y. Fainman, and B. Kanté, Lasing action from photonic bound states in continuum, *Nature* **541**, 196 (2017).
- [23] M.-S. Hwang, H.-C. Lee, K.-H. Kim, K.-Y. Jeong, S.-H. Kwon, K. Koshelev, Y. Kivshar, and H.-G. Park, Ultralow-threshold laser using super-bound states in the continuum, *Nature Communications* **12**, 4135 (2021).
- [24] S. Mohamed, J. Wang, H. Rekola, J. Heikkinen, B. Asamoah, L. Shi, and T. K. Hakala, Controlling topology and polarization state of lasing photonic bound states in continuum, *Laser & Photonics Reviews* **16**, 2100574 (2022).
- [25] R. Heilmann, G. Salerno, J. Cuerda, T. K. Hakala, and P. Torma, Quasi-BIC mode lasing in a quadrumer plasmonic lattice, *ACS Photonics* **9**, 224 (2022).
- [26] G. Salerno, R. Heilmann, K. Arjas, K. Aronen, J.-P. Martikainen, and P. Törmä, Loss-driven topological transitions in lasing, *Physical Review Letters* **129**, 173901 (2022).
- [27] L. Carletti, K. Koshelev, C. De Angelis, and Y. Kivshar, Giant nonlinear response at the nanoscale driven by bound states in the continuum, *Physical Review Letters* **121**, 033903 (2018).
- [28] K. Koshelev, Y. Tang, K. Li, D.-Y. Choi, G. Li, and Y. Kivshar, Nonlinear metasurfaces governed by bound

- states in the continuum, *ACS Photonics* **6**, 1639 (2019).
- [29] M. Minkov, D. Gerace, and S. Fan, Doubly resonant $\chi^{(2)}$ nonlinear photonic crystal cavity based on a bound state in the continuum, *Optica* **6**, 1039 (2019).
- [30] A. P. Anthur, H. Zhang, R. Paniagua-Dominguez, D. A. Kalashnikov, S. T. Ha, T. W. Maß, A. I. Kuznetsov, and L. Krivitsky, Continuous wave second harmonic generation enabled by quasi-bound-states in the continuum on gallium phosphide metasurfaces, *Nano Letters* **20**, 8745 (2020).
- [31] S. Joseph, S. Pandey, S. Sarkar, and J. Joseph, Bound states in the continuum in resonant nanostructures: an overview of engineered materials for tailored applications, *Nanophotonics* **10**, 4175 (2021).
- [32] A. Krasnok and A. Alú, Embedded scattering eigenstates using resonant metasurfaces, *Journal of Optics* **20**, 064002 (2018).
- [33] X. Wang, J. Duan, W. Chen, C. Zhou, T. Liu, and S. Xiao, Controlling light absorption of graphene at critical coupling through magnetic dipole quasi-bound states in the continuum resonance, *Physical Review B* **102**, 155432 (2020).
- [34] S. Xiao, X. Wang, J. Duan, T. Liu, and T. Yu, Engineering light absorption at critical coupling via bound states in the continuum, *J. Opt. Soc. Am. B* **38**, 1325 (2021).
- [35] R. M. Saadabad, L. Huang, and A. E. Miroshnichenko, Polarization-independent perfect absorber enabled by quasibound states in the continuum, *Physical Review B* **104**, 235405 (2021).
- [36] X. Zong, L. Li, and Y. Liu, Bound states in the continuum enabling ultra-narrowband perfect absorption, *New Journal of Physics* **25**, 023020 (2023).
- [37] J. Zhang, K. F. MacDonald, and N. I. Zheludev, Controlling light-with-light without nonlinearity, *Light: Science & Applications* **1**, e18 (2012).
- [38] X. Fang, K. F. MacDonald, and N. I. Zheludev, Controlling light with light using coherent metadevices: all-optical transistor, summator and inverter, *Light: Science & Applications* **4**, e292 (2015).
- [39] G. Pirruccio, M. Ramezani, S. R.-K. Rodriguez, and J. G. Rivas, Coherent control of the optical absorption in a plasmonic lattice coupled to a luminescent layer, *Physical Review Letters* **116**, 103002 (2016).
- [40] F. Monticone and A. Alú, Bound states within the radiation continuum in diffraction gratings and the role of leaky modes, *New Journal of Physics* **19**, 093011 (2017).
- [41] S. I. Azzam, V. M. Shalaev, A. Boltasseva, and A. V. Kildishev, Formation of bound states in the continuum in hybrid plasmonic-photonic systems, *Physical Review Letters* **121**, 253901 (2018).
- [42] Y. Liang, K. Koshelev, F. Zhang, H. Lin, S. Lin, J. Wu, B. Jia, and Y. Kivshar, Bound states in the continuum in anisotropic plasmonic metasurfaces, *Nano Letters* **20**, 6351 (2020).
- [43] R. Kolkowski, S. Kovaivos, and A. F. Koenderink, Trapping light in resonant metasurfaces for plasmon lasing, in *AIP Conference Proceedings*, Vol. 2300 (AIP Publishing LLC, 2020) p. 020060.
- [44] J. Xiang, Y. Xu, J.-D. Chen, and S. Lan, Tailoring the spatial localization of bound state in the continuum in plasmonic-dielectric hybrid system, *Nanophotonics* **9**, 133 (2020).
- [45] M. Meudt, C. Bogiadzi, K. Wrobel, and P. Görrn, Hybrid photonic-plasmonic bound states in continuum for enhanced light manipulation, *Advanced Optical Materials* **8**, 2000898 (2020).
- [46] S. Sun, Y. Ding, H. Li, P. Hu, C.-W. Cheng, Y. Sang, F. Cao, Y. Hu, A. Alú, D. Liu, *et al.*, Tunable plasmonic bound states in the continuum in the visible range, *Physical Review B* **103**, 045416 (2021).
- [47] Z.-L. Deng, F.-J. Li, H. Li, X. Li, and A. Alú, Extreme diffraction control in metagratings leveraging bound states in the continuum and exceptional points, *Laser & Photonics Reviews* **16**, 2100617 (2022).
- [48] A. Aigner, A. Tittl, J. Wang, T. Weber, Y. Kivshar, S. A. Maier, and H. Ren, Plasmonic bound states in the continuum to tailor light-matter coupling, *Science Advances* **8**, eadd4816 (2022).
- [49] Y. Zhou, Z. Guo, X. Zhao, F. Wang, Z. Yu, Y. Chen, Z. Liu, S. Zhang, S. Sun, and X. Wu, Dual-quasi bound states in the continuum enabled plasmonic metasurfaces, *Advanced Optical Materials* **10**, 2200965 (2022).
- [50] F. Cao, M. Zhou, C.-W. Cheng, H. Li, Q. Jia, A. Jiang, B. Lyu, D. Liu, D. Han, S. Gwo, *et al.*, Interaction of plasmonic bound states in the continuum, *Photonics Research* **11**, 724 (2023).
- [51] L. Novotny and N. Van Hulst, Antennas for light, *Nature Photonics* **5**, 83 (2011).
- [52] A. F. Koenderink, A. Alú, and A. Polman, Nanophotonics: Shrinking light-based technology, *Science* **348**, 516 (2015).
- [53] A. I. Kuznetsov, A. E. Miroshnichenko, M. L. Brongersma, Y. S. Kivshar, and B. Luk'yanchuk, Optically resonant dielectric nanostructures, *Science* **354**, aag2472 (2016).
- [54] H. Friedrich and D. Wintgen, Interfering resonances and bound states in the continuum, *Physical Review A* **32**, 3231 (1985).
- [55] S.-G. Lee, S.-H. Kim, and C.-S. Kee, Bound states in the continuum (BIC) accompanied by avoided crossings in leaky-mode photonic lattices, *Nanophotonics* **9**, 4373 (2020).
- [56] J. Tian, Q. Li, P. A. Belov, R. K. Sinha, W. Qian, and M. Qiu, High-Q all-dielectric metasurface: super and suppressed optical absorption, *ACS Photonics* **7**, 1436 (2020).
- [57] A. Christ, S. Tikhodeev, N. Gippius, J. Kuhl, and H. Giessen, Waveguide-plasmon polaritons: strong coupling of photonic and electronic resonances in a metallic photonic crystal slab, *Physical Review Letters* **91**, 183901 (2003).
- [58] S. Rodriguez, S. Murai, M. Verschuuren, and J. G. Rivas, Light-emitting waveguide-plasmon polaritons, *Physical Review Letters* **109**, 166803 (2012).
- [59] S. R.-K. Rodriguez, Classical and quantum distinctions between weak and strong coupling, *European Journal of Physics* **37**, 025802 (2016).
- [60] F. Alpegiani, N. Parappurath, E. Verhagen, and L. Kuipers, Quasinormal-mode expansion of the scattering matrix, *Physical Review X* **7**, 021035 (2017).
- [61] P. Lalanne, W. Yan, K. Vynck, C. Sauvan, and J.-P. Hugonin, Light interaction with photonic and plasmonic resonances, *Laser & Photonics Reviews* **12**, 1700113 (2018).
- [62] A. Krasnok, D. Baranov, H. Li, M.-A. Miri, F. Monticone, and A. Alú, Anomalies in light scattering, *Advances in Optics and Photonics* **11**, 892 (2019).

- [63] N. Shubin, V. Kapaev, and A. Gorbatshevich, Multimode resonances, intermode bound states, and bound states in the continuum in waveguides, *Physical Review B* **106**, 125425 (2022).
- [64] Z. Bai, C. Hang, and G. Huang, Classical analogs of double electromagnetically induced transparency, *Optics Communications* **291**, 253 (2013).
- [65] B. Zhen, C. W. Hsu, Y. Igarashi, L. Lu, I. Kaminer, A. Pick, S.-L. Chua, J. D. Joannopoulos, and M. Soljačić, Spawning rings of exceptional points out of Dirac cones, *Nature* **525**, 354 (2015).
- [66] M. Fleischhauer, A. Imamoglu, and J. P. Marangos, Electromagnetically induced transparency: Optics in coherent media, *Reviews of Modern Physics* **77**, 633 (2005).
- [67] N. Liu, L. Langguth, T. Weiss, J. Kästel, M. Fleischhauer, T. Pfau, and H. Giessen, Plasmonic analogue of electromagnetically induced transparency at the Drude damping limit, *Nature Materials* **8**, 758 (2009).
- [68] A. C. Overvig, S. Shrestha, and N. Yu, Dimerized high contrast gratings, *Nanophotonics* **7**, 1157 (2018).
- [69] A. C. Overvig, S. C. Malek, M. J. Carter, S. Shrestha, and N. Yu, Selection rules for quasibound states in the continuum, *Physical Review B* **102**, 035434 (2020).
- [70] S. Maurya, R. Kolkowski, M. Kaivola, and A. Shevchenko, Crosstalk reduction between closely spaced optical waveguides by using higher-order modes, *Physical Review Applied* **18**, 044077 (2022).
- [71] Z. Geng, K. Peters, A. Trichet, K. Malmir, R. Kolkowski, J. Smith, and S. Rodriguez, Universal scaling in the dynamic hysteresis, and non-Markovian dynamics, of a tunable optical cavity, *Physical Review Letters* **124**, 153603 (2020).
- [72] X. Yang, M. Yu, D.-L. Kwong, and C. W. Wong, All-optical analog to electromagnetically induced transparency in multiple coupled photonic crystal cavities, *Physical Review Letters* **102**, 173902 (2009).
- [73] H. M. Doleman, E. Verhagen, and A. F. Koenderink, Antenna-cavity hybrids: matching polar opposites for Purcell enhancements at any linewidth, *ACS Photonics* **3**, 1943 (2016).
- [74] K. G. Cognée, H. M. Doleman, P. Lalanne, and A. Koenderink, Cooperative interactions between nano-antennas in a high-Q cavity for unidirectional light sources, *Light: Science & Applications* **8**, 115 (2019).
- [75] H. M. Doleman, C. D. Dieleman, C. Mennes, B. Ehrler, and A. F. Koenderink, Observation of cooperative Purcell enhancements in antenna-cavity hybrids, *ACS Nano* **14**, 12027 (2020).
- [76] E. Verhagen, S. Deléglise, S. Weis, A. Schliesser, and T. J. Kippenberg, Quantum-coherent coupling of a mechanical oscillator to an optical cavity mode, *Nature* **482**, 63 (2012).
- [77] P. Törmä and W. L. Barnes, Strong coupling between surface plasmon polaritons and emitters: a review, *Reports on Progress in Physics* **78**, 013901 (2014).
- [78] Y.-X. Xiao, G. Ma, Z.-Q. Zhang, and C. T. Chan, Topological subspace-induced bound state in the continuum, *Physical Review Letters* **118**, 166803 (2017).
- [79] M. Amrani, S. Khattou, A. Talbi, A. Akjouj, L. Dobrzynski, B. Djafari-Rouhani, *et al.*, Friedrich-Wintgen bound states in the continuum and induced resonances in a loop laterally coupled to a waveguide, *Physical Review B* **106**, 125414 (2022).
- [80] W. Głowadzka, M. Wasiak, and T. Czyszanowski, True- and quasi-bound states in the continuum in one-dimensional gratings with broken up-down mirror symmetry, *Nanophotonics* **10**, 3979 (2021).
- [81] K. Luke, Y. Okawachi, M. R. Lamont, A. L. Gaeta, and M. Lipson, Broadband mid-infrared frequency comb generation in a Si_3N_4 microresonator, *Optics Letters* **40**, 4823 (2015).
- [82] I. H. Malitson, Interspecimen comparison of the refractive index of fused silica, *J. Opt. Soc. Am.* **55**, 1205 (1965).
- [83] P. B. Johnson and R.-W. Christy, Optical constants of the noble metals, *Physical Review B* **6**, 4370 (1972).
- [84] M. E. Stewart, C. R. Anderton, L. B. Thompson, J. Maria, S. K. Gray, J. A. Rogers, and R. G. Nuzzo, Nanostructured plasmonic sensors, *Chemical Reviews* **108**, 494 (2008).
- [85] D. Conteduca, G. S. Arruda, I. Barth, Y. Wang, T. F. Krauss, and E. R. Martins, Beyond Q : the importance of the resonance amplitude for photonic sensors, *ACS Photonics* **9**, 1757 (2022).
- [86] L. Zundel, J. R. Deop-Ruano, R. Martinez-Herrero, and A. Manjavacas, Lattice resonances excited by finite-width light beams, *ACS Omega* **7**, 31431 (2022).
- [87] S. Zou, N. Janel, and G. C. Schatz, Silver nanoparticle array structures that produce remarkably narrow plasmon lineshapes, *Journal of Chemical Physics* **120**, 10871 (2004).
- [88] L. Zundel and A. Manjavacas, Finite-size effects on periodic arrays of nanostructures, *Journal of Physics: Photonics* **1**, 015004 (2018).
- [89] Z. F. Sadrieva, I. S. Sinev, K. L. Koshelev, A. Samusev, I. V. Iorsh, O. Takayama, R. Malureanu, A. A. Bogdanov, and A. V. Lavrinenko, Transition from optical bound states in the continuum to leaky resonances: role of substrate and roughness, *ACS Photonics* **4**, 723 (2017).
- [90] M. S. Bin-Alam, O. Reshef, Y. Mamchur, M. Z. Alam, G. Carlow, J. Upham, B. T. Sullivan, J.-M. Ménard, M. J. Huttunen, R. W. Boyd, and D. K. Ultra-high- Q resonances in plasmonic metasurfaces, *Nature Communications* **12**, 974 (2021).
- [91] M. S. Bin-Alam, O. Reshef, R. N. Ahmad, J. Upham, M. J. Huttunen, K. Dolgaleva, and R. W. Boyd, Cross-polarized surface lattice resonances in a rectangular lattice plasmonic metasurface, *Optics Letters* **47**, 2105 (2022).
- [92] K. Koshelev and Y. Kivshar, Dielectric resonant metaphotonics, *ACS Photonics* **8**, 102 (2020).
- [93] A. Vaskin, R. Kolkowski, A. F. Koenderink, and I. Staude, Light-emitting metasurfaces, *Nanophotonics* **8**, 1151 (2019).
- [94] M.-S. Hwang, K.-Y. Jeong, J.-P. So, K.-H. Kim, and H.-G. Park, Nanophotonic nonlinear and laser devices exploiting bound states in the continuum, *Communications Physics* **5**, 106 (2022).
- [95] R. Kolkowski, T. K. Hakala, A. Shevchenko, and M. J. Huttunen, Nonlinear nonlocal metasurfaces, *Applied Physics Letters* **122**, 160502 (2023).
- [96] R. Kolkowski, Replication package for "Enabling infinite Q factors in absorbing optical systems", <https://doi.org/10.23729/cfe98559-2ca5-43c6-b8f3-b542f9ff94bb> (2023).